

Development of a Mechanical Model of the Lumens of the Male Reproductive Tract

By:

Olivia Luu, Hunter Smith, and Amber Assaid

Advisor:

Tim Barry

Word Count: 4831

Number of Figures: 5

Number of Tables: 1

Number of Equations: 3

Number of Supplements: 1

Number of References: 21

Development of a Mechanical Model of the Lumens of the Male Reproductive Tract

Olivia Luu¹, Hunter Smith¹, Amber Assaid¹, Tim Barry²

¹Department of Biomedical Engineering at the University of Virginia

²Contraline, Inc, Charlottesville, VA

Abstract

Contraline, Inc., is a biotechnology company based in Charlottesville, Virginia, developing a novel injectable, long-lasting, reversible male contraceptive called ADAM™. Their contraceptive is designed to inject a hydrogel into the vas deferens to physically occlude the flow of sperm from the testes into the ejaculatory duct. The male reproductive tract is poorly modeled outside of drawings and computer renderings, making it difficult for Contraline to perform proper injection testing with their hydrogel. The purpose of this research was to develop a mechanical model of the inner lumen, or the hollow center, of the tubule of the male reproductive tract. To model the reproductive tract and the inner lumen, mechanical properties testing, imaging, and extensive research were performed to determine the proper dimensions and mechanics. The model was then printed using a Formlabs Form 3 SLA printer with Elastic 50A resin, which best matched the experimentally derived Young's Modulus of the human vas deferens of 44.10 kPa with its own Young's Modulus of 45.55 kPa. The model was then encapsulated in Humimic Medical synthetic gelatin to mimic the abdominal tissue surrounding the vas deferens. Future work on this model will see a more extensive streamlining of the building process to increase production and better support Contraline's injection training to improve the efficacy of their contraceptive procedure.

Key words: contraceptive, lumen, mechanical modeling, Young's Modulus, Contraline

Introduction

In 2023, the prevalence of contraceptive use of any kind globally was estimated to be 65% with an estimate of 748 million¹ women using a modern method of contraception. Yet, one in five women have an unmet need for family planning, and women discontinue use within a year of contraception adoption due to various issues. In a 2020 study, over 1600 women were interviewed three to six months after oral contraceptive establishment and nearly 60% of women had discontinued contraceptive use by the end of six months². However, side effects only account for 33.8% of the women who discontinue use. The biggest reason for discontinuation was reported as logistical reasons, such as running out of pills, an inability to return to the

clinic, and forgetting to take the pill each night. With a high percentage of women discontinuing oral contraceptives, and only around 12% switching to another form of contraceptive³, weight begins to shift to men to take responsibility for family planning. Studies have shown an increase in men wanting to participate in family planning with a 26% jump from 2014 to 2021 in vasectomies⁴, or male sterilization, the only long-acting method of contraceptive for men currently on the open market. Vasectomies work by severing the vas deferens, a coiled tube that carries sperm out of the testes, and sealing the open ends to prevent sperm flow. After the overturning of Roe v. Wade in 2022, vasectomy rates have continued to rise, with some doctors reporting a

900% increase⁵ in vasectomy consultations. Insurance data has reported that the age range of men interested in vasectomies skews toward the younger generations⁶. Vasectomies however, are not meant to be reversible, or at the least, were not originally intended to be reversible. Yet, young men who may want to have a family in the future or men who may want to have more children in the future are being forced to rely on a contraceptive option that may not be temporary as there is a lack of reversible methods of male contraception on the market.

Contraline, Inc., a biotech start-up from Charlottesville, VA is developing a non-hormonal, long-lasting, reversible contraceptive for men, called ADAMTM, that works via vas-occlusion, utilizing advances in hydrogel technology. This proprietary hydrogel is implanted into the vas deferens via a minimally invasive, outpatient procedure, designed to block the travel of sperm out of the vas deferens and into the ejaculatory duct, similar to a vasectomy, without affecting sensation or ejaculation. The sperm that becomes blocked naturally degrade and are reabsorbed into the body⁷. After a lifespan on the scope of years, will either liquify or be removed via another outpatient procedure, and sperm flow through the vas deferens will be resumed. ADAMTM offers a reversible method for men, decreasing the need of men to rely on vasectomies for family planning.

The success of the hydrogel not only depends on the ability of the hydrogel to block the vas deferens, but also on the accuracy of the technicians, doctors, or any users of the contraceptive to properly inject the hydrogel. This requires consistent practice with the injection device and a model to inject into. Currently, injection testing is typically performed with plastic tubing. The tubing however, lacks the proper mechanical properties of the vas deferens. In general, the human male reproductive tract is poorly modeled outside of drawings and computer renderings, specifically the ampulla, an enlargement of the vas deferens that serves as a reservoir⁸ for sperm, and the ejaculatory duct, a tube that moves through the prostate to pick up fluid which empties into the urethra. This lack of representation makes it difficult to perform accurate experiments with a vas-occluding contraceptive such as ADAMTM.

The first aim of this project was to develop a model that mimics the inside of the male reproductive tract, from where the vas deferens meets the epididymis to the start of the ejaculatory duct. The model was informed by various drawings and digital renderings of the human vas deferens and literature describing the dimensions of the respective parts of the reproductive tract. The second aim of this project was to fabricate the model with some elastic or viscoelastic material that matches the dynamic response of each respective vessel when pressurized or manipulated. Subaims were added to the fabrication of the model to be scalable, repeatable, and producible in quantities of greater than ten, requiring less than ten hours of work per model creation, including assembly.

Materials and Methods

Model Material Selection

Previous model iterations were made from polydimethylsiloxane (PDMS) resin⁹. PDMS is used to create models via an application known as soft lithography¹⁰. Soft lithography makes a three-dimensional structure out of PDMS from a master mold. The downside to a material such as PDMS is that it is restricted to solid objects. Since the resin is poured into the mold, unless an object is placed in the center, the model is likely to be entirely solid. The previous capstone group working with Contraline worked around this issue by placing a 20 ga wire through the center of the mold. This however, will not work with our model, as it is modeling the entire tract which curves, requiring a non-linear core.

The chosen approach for this model, which dictates the model selection, is stereolithography (SLA), a form of additive manufacturing which utilizes UV-photopolymerization. A UV laser runs over a layer of liquid resin to cure it in selected areas dictated by the tool path. After the completion of one layer, another layer of resin is coated on top of the cured layer and the laser process is repeated until the part is complete. This method of model creation will allow for the hollow center, lumen, of the male reproductive tract. Given this new criteria, the chosen material for our model was either Formlabs Elastic 50A or Flexible 80A resin, where the A refers to the shore hardness, ranging from very soft mold rubbers to semi-rigid plastics¹¹. The 50

and 80 refer to the hardness on the given scale, with 50 being between a pencil eraser and a bottle nipple, and 80 having a similar hardness to a leather belt. These two types of resin are the only two sold by Formlabs, a 3D printing technology developer and manufacturer, that have elastic or viscoelastic properties. Elastic 50A was chosen for its similarity in Young's Modulus to the samples of human vas deferens tested using the nanoindenter, as outlined in the *Nanoindentation* section of the results.

Model Design

We took to literature to determine the dimensions of each section of the reproductive tract, which encompasses the vas deferens, ampulla, and ejaculatory duct. The original design also included the epididymis and the testicle. These two components were removed from the final design (Figure 1) as they are not the most important to the testing of the contraceptive device, and their removal helps to streamline the fabrication process, keeping it short and cost-effective.

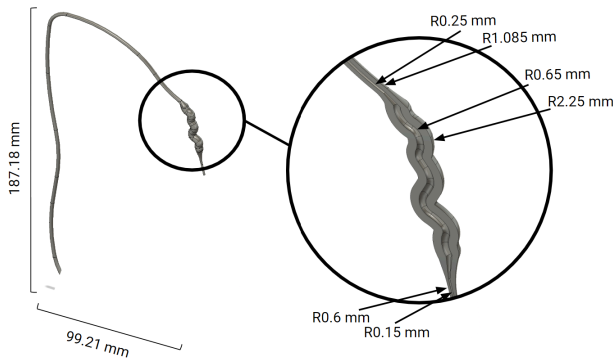


Figure 1. Final Lumen Model Design. The final design was created in Autodesk Fusion 360[®] using a combination of splines, curves, and pipes. After designing, the model was then split in half along the y-axis to create two mirror-image pieces.

In a paper by Liu et al., 210 samples of vas deferens from volunteer vasectomy patients, the mean equivalent-round outer and inner diameters were determined to be 2.17 ± 0.2 mm and 0.56 ± 0.08 mm, respectively. The values used for the vas deferens of our model were 2.17 mm and 0.50 mm, respectively. Since the ampulla is poorly represented in literature, we consulted our advisor Tim Barry, and determined the inner and outer diameters of the ampulla to be 1.3 mm and 4.5 mm, respectively based on Contraline's previous

work in the cadaver model. Regarding the ejaculatory duct, literature states the inner diameter to be between 0.2 and 0.3 mm¹² and the outer diameter to be between 0.9 and 1.4 mm¹³. For the best results in printing, we chose an inner diameter of 0.3 mm and an outer diameter of 1.2 mm.

When designing the model, we were restricted by certain features of the Formlabs Form 3 printer, used for the printing of the model. The Form 3 prints in layers of 25, 50, or 100 microns, with feature detail down to 0.3 mm¹⁴. However, the printer is not ideal for parts with walls thinner than 0.5 mm. The 0.3 mm feature detail of the printer is beneficial as the inner diameter of our model sits at 0.5 mm. One limitation of printing with resin is the potential for excess resin build up. When designing something with such a small hole, resin can get trapped and become cured by the UV laser. This would result in a solid model instead of a hollow model, which is required to indicate the lumen itself. To work around these issues, the model was designed in two mirrored halves to be combined in post-production.

Preparation of Human Vas Deferens Samples

Three samples of human vas deferens were provided from Contraline as an output of some Virginia Catalyst grant work between Contraline and UVA Health Department of Urology. The samples were transported to the UVA Biorepository and Tissue Research Facility where they were sectioned into 4 μ m sections and placed onto charged histological slides. The samples were stained using a hematoxylin and eosin (H&E) stain to obtain a cosmetic view of the tissue. Once stained, the sections were imaged using a Leica Thunder brightfield microscope in the Peirce-Cottler Lab. Image analysis was performed using ImageJ. The tissue sectioning process resulted in the inner lumen being compressed and deviating from a circular geometry. Therefore, the circumference of the inner and outer lumen was determined and the inner and outer diameter were found using equation 1, where C is circumference and d is the diameter of the lumens.

$$C = \pi d \quad (\text{Equation 1})$$

Determination of Mechanical Properties of Materials

Tensile Testing

In order to determine a baseline for the mechanical properties, tensile testing was performed on five different materials. Two samples of three types of tubing, and two samples of Elastic 50A, and four samples of previously prepared and tested samples of canine vas deferens were provided by Contraline. The canine vas deferens samples were removed from the -80°C freezer to thaw and flat ends were cut from each of the four samples to achieve the closest in shape possible to the original, untested canine vas deferens. Testing was performed using an Instron 3400 Series single column system Universal Tensile Machine¹⁵ that can provide up to 5 kN of tensile or compressive strength.

After documenting the length, width, and thickness of each material for later calculations, each sample was loaded into the Instron to collect the displacement (mm) and the force load (kN). To calculate the mechanical properties, the displacement or extension was plotted against the force load to create a stress-strain curve. The stress (σ) and the strain (ϵ) were calculated using Equations 2 and 3, respectively. Young's Modulus (E), Ultimate Tensile Strength (UTS), and stiffness at 10% strain were all calculated using MATLAB's `getpts()` function (Figure S1). Graphs were extrapolated from ten samples of the previous capstone group's tensile testing data on canine vas deferens, using the same technique to compare the Young's Modulus to the stiffness at 10% strain, specifically, which is the physiologically relevant range that Contraline is interested in.

$$\sigma = \text{load}/(\text{width} * \text{thickness}) \quad (\text{Equation 2})$$

$$\epsilon = \text{displacement}/\text{length} \quad (\text{Equation 3})$$

Nanoindentation

Three samples of human vas deferens were provided by Contraline. The samples were obtained by Contraline from the UVA Health Department of Urology via the previously mentioned Virginia Catalyst grant. The samples were ~0.5 cm in length and therefore could not be tested for mechanical properties using an Instron. An OpticsII Piuma Nanoindenter in the Caliri Lab was used to obtain mechanical properties of the vas deferens samples. Using the nanoindenter, values for Young's Modulus, Storage Modulus, and Loss Modulus were

obtained. Two samples of canine vas deferens were provided by Contraline from a previous project and were used as a trial to test the feasibility of testing human samples. After successful trials with canine samples, human samples were tested. Finally, Elastic 50A and Flexible 80A resins were tested for comparison of the printed material to tissue. The nanoindenter tip had a Geofactor in air of 3.68, stiffness of 0.46 N, and tip radius of 50.5 μm .

The tip was first calibrated in PBS, and the vas deferens sample was secured to a 6 cm petri dish using adhesive. The petri dish was filled with PBS and placed under the nanoindenter. The nanoindenter tip was aligned with the sample. A dynamic mechanical analysis (DMA) was performed at a frequency of 1 Hz. Finally, the sample was realigned with the nanoindenter tip at another location for DMA to be performed. This process was repeated for five total points per sample and for two samples of the resin samples.

Tissue Material Selection

Tissue Anatomy

To encapsulate the printed model, Humimic Medical Synthetic Gelatin was used to simulate lower abdominal tissue surrounding the pelvic region. The tissue chosen for replication was the Rectus Abdominis (RA) muscle due to its anatomical position in the male pelvic region, beginning at the pubic symphysis and running vertically up the abdominal midline. The pubic symphysis joint is situated at the bottom of the pelvis, joining the two pelvic bones¹⁶. The ductus deferens initially travels along the anterior side of the pelvic bones before curving medially toward the posterior and approaching the urinary bladder. From there, it wraps around the side of the bladder, passing superior to the ureters before descending along the back of the bladder towards the prostate gland. As it reaches the ampulla region, the ductus deferens widens before tapering again and merging with the seminal vesicles at the ejaculatory duct¹⁷. This was the region of interest in the male reproductive tract, all residing beneath skin, subcutaneous tissue, and abdominal muscles including the RA.

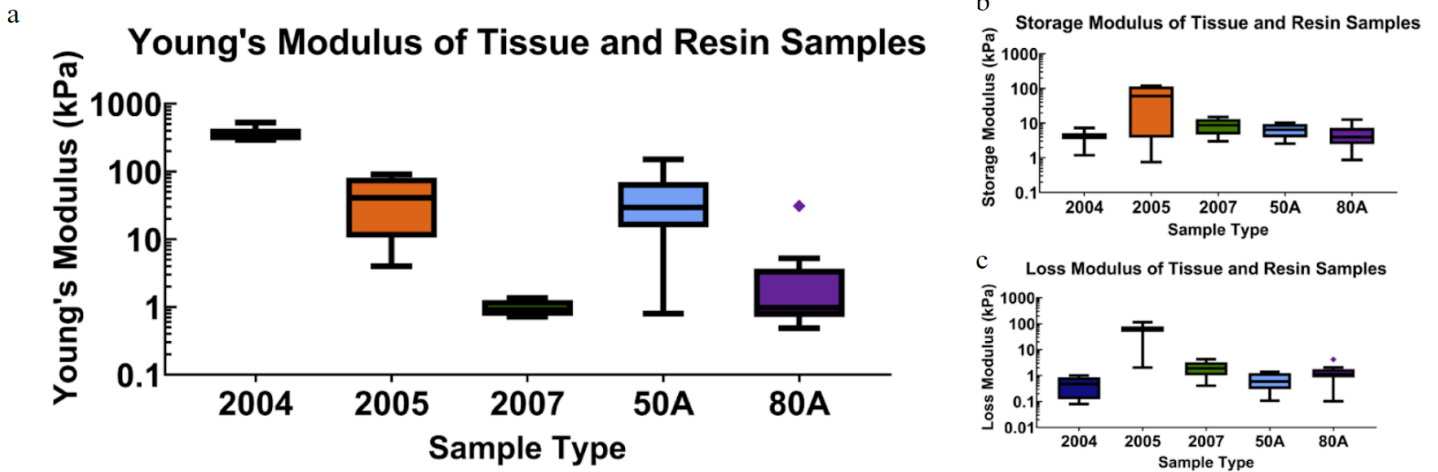


Figure 2. Graphs of nanoindentation results. Graphs were created depicting the values for each of the three test results showing the mean and standard deviation. a. Graph of Young's Modulus of the three human vas deferens tissue samples and the two samples of Formlabs resin. The graph shows the similarity in Young's Modulus between Sample 2005 and Elastic 50A resin. b. Graph of Storage Modulus of the tissue and resin samples. c. Graph of Loss Modulus of the tissue and resin samples. Each graph is on a logarithmic scale.

Material Properties

Mechanical testing of abdominal muscles has been done on cadaver muscle tissue to determine tensile properties. Uniaxial tensile testing was performed on cadaveric fresh-never-frozen (FNF) Rectus Abdominis tissue to identify its Elastic Modulus at 0.19 MPa¹⁸. Using the Humimic Medical Gelatin Technical Data Sheet, the gel identified that most closely aligns with RA Elastic Modulus determined from literature was Gel #5. This gel was chosen because it closely mimics real tissue values with a Young's Modulus of 0.21 MPa¹⁹. To determine accurate anatomical placement of the model, thickness of abdominal skin, subcutaneous fat, and RA muscle was researched. Values obtained from literature indicate total mean thickness of subcutaneous fat and RA muscle tissue in the male abdomen was 0.808 cm and 2.12 cm, respectively²⁰. The mean thickness of male abdominal dermis was determined to be 0.21 cm²¹. In sum, 3.14 cm combining these layers. Fascia, extraperitoneal fat and blood vessels and nerves lie between these layers and the male reproductive tract.

Results

Property Analysis

Nanoindentation

Nanoindentation was performed on three human vas deferens samples, Samples 2004, Sample 2005, and Sample 2007, and two resin types, Elastic 50A and Flexible 80A resins. The mean and standard deviation of Young's Modulus, Storage Modulus, and Loss Modulus

were obtained. The Young's Modulus of the samples were 391.1 ± 122.8 kPa for Sample 2004 ($n = 3$), 44.1 ± 36.6 kPa for Sample 2005 ($n = 4$), 1.0 ± 0.3 kPa for Sample 2007 ($n = 4$), 45.6 ± 53.6 kPa for Elastic 50A ($n = 6$), and 4.8 ± 10.0 kPa for Flexible 80A ($n = 9$). The Storage Modulus of samples were 4.2 ± 4.3 kPa for Sample 2004 ($n = 2$), 59.7 ± 61.4 kPa for Sample 2005 ($n = 4$), 8.9 ± 4.6 for Sample 2007 ($n = 5$), 6.6 ± 2.9 kPa for Elastic 50A ($n = 6$), and 5.1 ± 3.8 kPa for Flexible 80A ($n = 9$). The Loss Modulus of samples was 0.5 ± 0.4 kPa for Sample 2004 ($n = 5$), 59.3 ± 56.0 kPa for Sample 2005 ($n = 3$), 2.1 ± 1.4 kPa for Sample 2007 ($n = 5$), 0.7 ± 0.5 kPa for Elastic 50A ($n = 8$), and 1.4 ± 1.1 kPa for Flexible 80A ($n = 10$). (Figure 2)

Tensile Testing

The main property that we aimed to get out of tensile testing was the Young's Modulus of each of the synthetic materials and the vas deferens. When performing this testing, the values for Young's Modulus varied drastically from the values obtained via nanoindentation. For the samples of Elastic 50A, we obtained a value of 1.5 MPa, which when compared to the value from nanoindentation, we noticed an almost 200% difference between the two testing methods. In the end, we chose to go with the values from nanoindentation as the samples of human vas deferens were tested with this method, and we wanted to maintain as much consistency as possible. Though we are unsure where this discrepancy comes from, it is likely due to possible slippage of materials or

a difference in the curing time of the resin samples used for nanoindentation and those used for tensile testing.

We also wanted to determine the stiffness of the material at a 10% strain rate. Tim noted that when working with elastic biological materials such as the vas deferens, the stiffness at 10% strain is the most physiologically relevant of the deformation of the material than Young's Modulus as many tissues have non-linear properties. To keep consistency, we analyzed the stiffness at 10% strain for the synthetic materials in addition to the biological canine samples. For the synthetic materials, we noticed very little difference between the stiffness at 10% strain and the Young's Modulus. For the Formlabs Elastic 50A (n=2), the Young's Modulus was 1.5 MPa, while the stiffness was 1.7 MPa. For one of the types of tubing called Eldon James (n=2), the values came out to be 6.2 MPa and 6.9 MPa, respectively. However, we noticed a large difference when comparing the biological canine vas deferens tissue. This confirmed the suspicion that Young's Modulus is not the most accurate representation of the modulus of elasticity of the biological tissue.

Sample	Young's Modulus	Stiffness at 10% Strain	Percent Difference
Canine Vas Deferens 2	19.06	11.52	49.31
Canine Vas Deferens 3	9.35	N/A	N/A
Canine Vas Deferens 4	54.84	60.32	9.52
Canine Vas Deferens 5	0.18	0.01	178.95
Canine Vas Deferens 6	7.1554	3.71	63.42
Canine Vas Deferens 7	28.4399	4.4827	145.54
Canine Vas Deferens 8	13.5051	12.2695	9.588
Canine Vas Deferens 9	33.4958	14.5487	78.87
Canine Vas Deferens 10	29.5395	9.9642	99.1
Canine Vas Deferens 11	18.4857	21.8126	16.51

Table 1. Comparison of Young's Modulus and Stiffness at 10% strain of canine vas deferens samples. Values for Young's Modulus and stiffness at 10% strain were extrapolated from data collected by a previous capstone group. All values were calculated in MPa.

Histology Imaging

Histology, Imaging, and image analysis was performed on three human vas deferens samples: Samples 2004, Sample 2005, and Sample 2007 (Figure 3). The mean and standard deviation for the inner and outer diameter of the lumens of the vas deferens were determined. The inner diameters of the samples were 0.475 ± 0.142 mm for Sample 2004 (n = 4), 0.387 ± 0.128 mm for Sample 2005 (n = 4), and 0.490 ± 0.047 mm for Sample 2007 (n = 4). The outer diameters of the samples were 3.456 ± 0.146 mm for Sample 2004 (n = 4), 2.548 ± 0.065 mm for Sample 2005 (n = 4), and 4.725 ± 0.086 mm for Sample 2007 (n = 4).

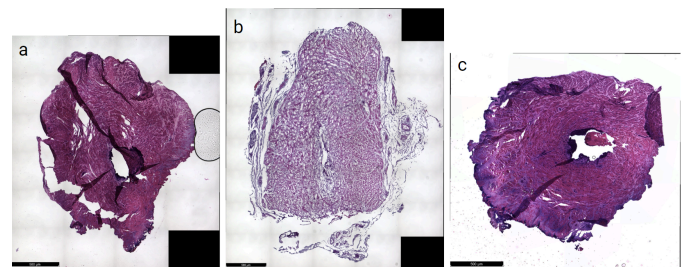


Figure 3. Histology images of three human vas deferens samples. Hematoxylin and Eosin (H&E) staining was performed on these three samples of human vas deferens and the circle-equivalent diameters were extrapolated from these images. The black scale bar in the bottom left corner measures 500 μ m.

Model Creation

The Reproductive Tract

After printing the model using the Formlabs Form 3 SLA printer, the model was removed from the build plate and placed into a bath of isopropyl alcohol for five minutes with constant agitation (Figure 4). After five minutes, the model was promptly removed and the supports were carefully taken off of the model and placed in waste containers. The support posts are filed down and 24 ga dead soft brass wire is placed in the model trough. An even layer of uncured resin from the resin tank is added to the model and the top is carefully placed and aligned on top. The model is wrapped with floss then cured for 60 minutes at 70°C , and the wire is removed.

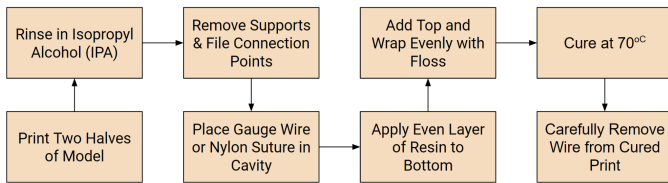


Figure 4. Model Assembly Process. A flow chart outlining the process for assembling the two halves of the model to put together one complete model of the lumen of the reproductive tract.

Tissue Encapsulation

450g of Humimic Medical Synthetic Gelatin #5 was cut into small cubes and placed into a glass dish with dimensions to fit 18.8 cm x 10 cm x 5 cm. The glass dish was placed inside an oven at 120° F for 50 minutes until the gel reached a liquid-like state. After it was removed from the oven, forceps were used to situate the model inside the heated gel. To estimate the position of the epididymis end and the ejaculatory duct end of the printed model, it was assumed the minimum thickness must be 3.14 cm. Accounting for all previously mentioned tissue, the gel tissue had a thickness of 5.5 cm. From the anterior position, the epididymis end is less deep than that of the ejaculatory duct end. The epididymis end of the model was placed 3 cm into the gel and the ejaculatory duct end was placed 5 cm into the gel to maintain anatomical position in relation to lower abdominal tissue (Figure 5).

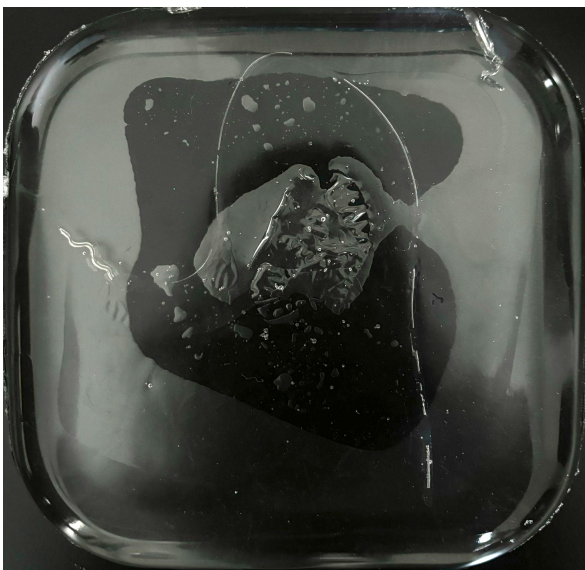


Figure 5. Final Encapsulated Model. The model of the male reproductive tract was encapsulated in Humimic Medical gelatin to represent the tract within abdominal tissue.

After the model was placed inside the gel, the glass dish was placed back into the oven at the same temperature for 30 minutes to remove air bubbles. It was removed and cooled until the gel reverted to a solid-like state. Using gloves, the encapsulated model was removed from the dish.

Discussion

Impact

The results of this project, especially the mechanical testing of the human vas deferens will help bring an insight into the structure and function of the male reproductive tract. With the samples of vas deferens from vasectomies, we were able to determine an approximate Young's Modulus for the vas deferens, which came out to be 44.1 ± 36.6 kPa. This high Young's Modulus may help researchers understand stiff, yet elastic properties of the vas deferens. With this model, we hope that technicians in clinics around the world can experience working with Contraline's hydrogel contraceptive, and ADAM can become the next contraceptive of choice for men. Since the male reproductive tract is so poorly represented physically, as mentioned in our problem statement, we hope that our model can serve as a new reference for the shape and size of the lumen and the overall structure of the male reproductive tract.

Limitations

We were met with significant challenges in regards to sample mechanical testing. With samples of human vas deferens, it is important that the tissue remains at a stable temperature. This required the acquisition of dry ice to transport the samples from Contraline to each of the respective labs for staining and testing. We also ran into trouble performing nanoindentation as we were unable to meet with the lab for several weeks due to logistical issues. In working with the samples of human vas deferens, we noticed that two of the samples, Sample 2004 and Sample 2007, were abnormal. Sample 2004 lacked much moisture when we prepared it for testing, and Sample 2007 was packed in some sort of liquid preservative. We believe that these abnormalities skewed the results of our nanoindentation testing, as the values for Young's Modulus of Sample 2004 and Sample 2007 were abnormally high and low, respectively. Given this,

we used Sample 2005 as our baseline for choosing our model material. It would have been more accurate to have had more samples of human vas deferens similar to the state of Sample 2005.

In printing the lumen model, we were extremely limited by the capabilities of the SLA printer. Form 3s are quite old in comparison to the other printers released by Formlabs so it lacks much of the precision and quality that other printers have. We were also limited by the material that we could use. We only had a choice between two types of elastic and viscoelastic resin, and while neither were perfect in modeling the properties of the vas deferens, Elastic 50A resin came the closest. We also found that males aged 19-32 have a mean subcutaneous fat layer of 1.33 cm, but this thickness increases in age groups 32-45 (2.36 cm) and 45-58 (2.60 cm), thus the thickness of the simulated tissue is not an accurate representation of the population of men as a whole who may be receiving this contraceptive. RA tissue thickness also varies, decreasing with increasing age¹⁸.

Future Work

Regarding the limitation of the Formlabs printers, in the future, printing and assembly can be done with a newer SLA printer with higher refinement and precision. The possibility of using a different type of SLA printer other than Formlabs could be explored which could widen the options for materials, finding one that is better suited to represent the mechanical properties of the human vas deferens. Wiring can also be cut to fit the exact dimensions of the model, removing the difficulty involved in carefully placing the wire into the model trough. However, with the possibility of using a higher resolution printer, the assembly process could be removed altogether, and the model can be printed as one complete piece with an intact inner lumen. To ameliorate the limitation involving the range of thicknesses of subcutaneous fat of men, we can perform replications of tissue for different age groups, taking average abdominal tissue thickness by age group into account. With a bigger volume and surface area of simulated tissue, we may be able to place multiple models of the lumen into a single block and clinicians and other trainees will be able to practice on multiple different models of different age groups.

These limitations aside, we hope that in the future, our model is printed in larger quantities to aid Contraline with their testing. We hope that this model can help to optimize hydrogel injections using it as a method to practice pressure and control. We also see possible applications of our model in the future for hydrogel porosity testing, determining the flow of fluid through the hydrogel, lower abdominal muscle testing, using the Humimic Medical synthetic gelatin, and possible hydrogel removal or exchange testing. In the end, we hope that our model can help make a small step forward in revolutionizing the world of male contraceptives.

End Matter

Author Contributions and Notes

Olivia Luu, Hunter Smith, and Amber Assaid performed sample testing, created CAD designs, fabricated prototypes, trialed assembly methods, and wrote the report. Tim Barry provided advising regarding model creation and properties testing, and aided in figure designs.

Acknowledgments

We would like to thank the entire Contraline team, especially Tim Barry, their Director of Engineering and Product Transfer, for the help on this work and the use of the equipment and facilities. Thank you to the UVA Health Department of Urology, in particular Dr. Ryan Smith, and the Virginia Catalyst grant program that allowed for us to do mechanical testing on appropriate tissues. Thank you to Dr. Steven Caliarri and his research team as well as Lloyd McMahon for the help in testing the properties of the samples of human and canine vas deferens. Thank you to the UVA Biorepository and Tissue Research Facility for aiding in the staining of the vas deferens sample, and lastly thank you to Dr. Timothy Allen and the entire Capstone teaching team for their support throughout the whole process.

References

1. Priorities for research on family planning impact: recommendations of a WHO Think Tank meeting - PMC. Accessed April 29, 2024.

- <https://www.ncbi.nlm.nih.gov/pmc/articles/PMC10565323/>
- Westhoff CL, Heartwell S, Edwards S, et al. Oral Contraceptive Discontinuation: Do Side Effects matter? *Am J Obstet Gynecol*. 2007;196(4):412.e1-412.e7. doi:10.1016/j.ajog.2006.12.015
 - Simmons RG, Sanders JN, Geist C, Gawron L, Myers K, Turok DK. Predictors of contraceptive switching and discontinuation within the first 6 months of use among Highly Effective Reversible Contraceptive Initiative Salt Lake study participants. *Am J Obstet Gynecol*. 2019;220(4):376.e1-376.e12. doi:10.1016/j.ajog.2018.12.022
 - Trends in the Vasectomy Rate Among Privately Insured Men Aged 18–64 in the United States Between 2014 and 2021 - Urology. Accessed April 29, 2024. [https://www.goldjournal.net/article/S0090-4295\(23\)00522-8/abstract](https://www.goldjournal.net/article/S0090-4295(23)00522-8/abstract)
 - What Men Need to Know About Getting a Vasectomy. Fatherly. Published July 15, 2022. Accessed April 29, 2024. <https://www.fatherly.com/life/questions-about-getting-vasectomy>
 - Vasectomies rose by 29% in the three months after the end of Roe. Accessed April 29, 2024. <https://www.economist.com/united-states/2023/05/25/vasectomies-rose-by-29-in-the-three-months-after-the-end-of-roe>
 - Vasectomy. Published October 12, 2022. Accessed May 5, 2024. <https://www.hopkinsmedicine.org/health/treatment-tests-and-therapies/vasectomy>
 - Jones RE, Lopez KH. Chapter 4 - The Male Reproductive System. In: Jones RE, Lopez KH, eds. *Human Reproductive Biology (Fourth Edition)*. Academic Press; 2014:67-83. doi:10.1016/B978-0-12-382184-3.00004-0
 - Raghu V. *Optimizing Current Delivery Methods of a Male Nonhormonal Contraceptive in the Form of a Hydrogel and Gender Inequality in Reproductive Health and the Prolonged Development of Male Contraception*. [object Object]; 2023. doi:10.18130/JD32-0877
 - Rapid Prototyping - ScienceDirect. Accessed April 29, 2024. <https://www.sciencedirect.com/science/article/abs/pii/B0080431526014388>
 - windmill. Durometer Shore Hardness Scale Explained | AeroMarine. Aeromarine Products Inc. Published July 30, 2020. Accessed April 29, 2024. <https://www.aeromarineproducts.com/durometer-shore-hardness-scale/>
 - Lv KL, Sun WG, Zhang TB, et al. Efficacy analysis of 26 cases of ejaculatory duct obstruction treated by prostatic utricle neck endoscopy. *Front Surg*. 2022;9. doi:10.3389/fsurg.2022.1031739
 - Li YF, Wang MS, Li BJ. AB213. Study on the applied anatomy of the ejaculatory duct region. *Transl Androl Urol*. 2016;5(Suppl 1):AB213. doi:10.21037/tau.2016.s213
 - Form 3 SLA 3D Printer – The James and Anne Duderstadt Center. Accessed April 29, 2024. <https://www.dc.umich.edu/partners-2/ground-connections-dmc/fabrication-studio/form-3/>
 - 3400 Series Universal Testing Systems. Accessed April 29, 2024. <https://www.instron.com/en/products/testing-systems/universal-testing-systems/low-force-universal-testing-systems/3400-series>
 - Anatomy, Abdomen and Pelvis: Abdominal Wall - StatPearls - NCBI Bookshelf. Accessed April 30, 2024. <https://www.ncbi.nlm.nih.gov/books/NBK551649/>
 - The Ductus Deferens: Anatomy and 3D Illustrations. Innerbody. Accessed April 30, 2024. https://www.innerbody.com/image_repmov/repo26-new2.html
 - Kriener K, Lala R, Homes RAP, et al. Mechanical Characterization of the Human Abdominal Wall Using Uniaxial Tensile Testing. *Bioengineering*. 2023;10(10). doi:10.3390/bioengineering10101213
 - Humimic-Medical-Gelatin-Technical-Sheet.pdf. Accessed April 30, 2024. <https://humimic.com/wp-content/uploads/2020/06/Humimic-Medical-Gelatin-Technical-Sheet.pdf>
 - E Abbas A, Hatem Alrawi M, Mahjoub Saeed EA. Assessment of Anterior Abdominal Wall Layers Thickness under the influence of Age and Sex, Using Computed Tomography Imaging in Ibn-Sina Hospital, Khartoum, Sudan 2021. *Arch Clin Biomed Res*. 2022;06(06). doi:10.26502/acbr.50170311

21. Derraik JGB, Rademaker M, Cutfield WS, et al.
Effects of Age, Gender, BMI, and Anatomical Site on
Skin Thickness in Children and Adults with Diabetes.
PLoS ONE. 2014;9(1):e86637.
doi:10.1371/journal.pone.0086637

Supplemental Material

```
length = a;  
width = b;  
thickness = c;  
values = readtable("name_of_data_file");
```

```
displacement = table2array(values(:,2));  
load = table2array(values(:,3));  
stress = load/(width*thickness);  
strain = displacement/length;  
plot(strain, stress);
```

```
[x,y] = getpts; %select four points. One at 10%  
strain, two on the linear portion of the graph, and  
one on the maximum point on the graph
```

$$E = (y(3)-y(2))/(x(3)-x(2))$$

$$UTS = y(4)/x(4)$$

$$ten = (y(1)-0)/(x(1)-0)$$

Supplemental Figure 1. MATLAB code to generate stress-strain curves. MATLAB code was adapted from code used in a group member's third year IDEAs lab to generate a plot of stress vs. strain and calculate values for the Young's Modulus (E), the Ultimate Tensile Strength (UTS), and the stiffness at 10% strain (ten).